Chemosphere 271 (2021) 129571

Contents lists available at ScienceDirect

Chemosphere

journal homepage: www.elsevier.com/locate/chemosphere

Evaluation of the effectiveness of VOC-contaminated soil preparation based on AHP-CRITIC-TOPSIS model

Yuan Li [a, b], Mingli Wei [a, c, d, e, *], Lei Liu [a, c, d], Bowei Yu [f], Zhiwei Dong [a, b], Qiang Xue [a, c, d, **]

[a] State Key Laboratory of Geomechanics and Geotechnical Engineering, Institute of Rock and Soil Mechanics, Chinese Academy of Sciences, Wuhan, 430071, China
[b] University of Chinese Academy of Sciences, Beijing, 100049, China
[c] IRSM-CAS/HK Poly U Joint Laboratory on Solid Waste Science, Wuhan, 430071, China
[d] Hubei Province Key Laboratory of Contaminated Sludge and Soil Science and Engineering, Wuhan, China
[e] Jiangsu Institute of Zoneco Co., Ltd., Yixing, 214200, China
[f] School of Civil Engineering, University of Sydney, 2008, Australia

HIGHLIGHTS

- Homogeneity (CV) and recovery (RR) are used to evaluate preparation effectiveness.
- AHP-CRITIC-TOPSIS model obtains the optimal method by scoring (highest score, 0.857).
- Applying optimal method to natural soil is feasible, its recovery is often high.
- Soil adsorption-related property has effect on sample preparation ($r = 0.848–0.991$).

GRAPHICAL ABSTRACT

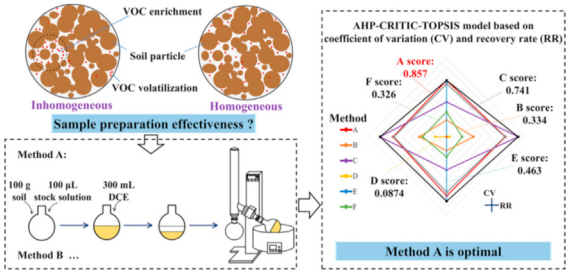

ARTICLE INFO

Article history:
Received 19 September 2020
Received in revised form
29 December 2020
Accepted 4 January 2021
Available online 7 January 2021

Handling Editor: Xiangru Zhang

Keywords:
VOC-Contaminated soil
Homogeneity
AHP-CRITIC-TOPSIS model
Adsorption effect

ABSTRACT

Currently, several methods have been adopted for the laboratory preparation of artificial volatile organic compound (VOC) contaminated soils (VCSs). However, it remains unclear whether the prepared contaminated soils are homogenous. In this study, two representative VOCs, toluene and perchloroethylene, were separately mixed with a kaolin-based soil using six preparation methods. Thereafter, the homogeneity and recovery of the contaminated kaolin prepared using these methods were determined and analyzed. The six procedures were quantitatively assessed according to the comprehensive evaluation mathematical model (AHP-CRITIC-TOPSIS), and the final score order of the different procedures was: A > C > E > B > F > D. Additionally, the qualitative evaluation of the procedures was performed based on the phase transformation and mass transfer during the mixing processes. Based on these discussions, method A, which was considered to be optimal, was then adopted for further investigations with various natural soils. The results showed that this optimal method could be applied to natural soils and revealed that the adsorption-related characteristics of natural soils, including total organic carbon, specific surface area, pore volume, pH, plastic limit, particle size, and mineral composition, influenced the homogeneity and recovery through mass transfer. In addition, it was also observed that the chemical

* Corresponding author. Institute of Rock and Soil Mechanics, Chinese Academy of Sciences, China.
** Corresponding author. Institute of Rock and Soil Mechanics, Chinese Academy of Sciences, China.
E-mail addresses: liyuan18@mails.ucas.ac.cn (M. Wei), qxue@whrsm.ac.cn (Q. Xue).

https://doi.org/10.1016/j.chemosphere.2021.129571

properties of VOCs, including molecular structure, vapor pressure, and the octanol/water partition coefficient, could also affect the effectiveness of sample recovery. Through this study, researchers can prepare VCSs with excellent homogeneity and low loss rates to conduct standardized tests for technology development.

1. Introduction

Volatile organic compound (VOC) contamination in soils has become a worldwide concern (Mdlovu et al., 2019; Xu et al., 2019). A variety of remediation technologies, e.g., soil vapor extraction, chemical oxidation, and bioremediation have been developed and applied in practice to resolve this issue (Agarwal and Liu, 2015; Lim et al., 2016; Tan et al., 2020; Vidonish et al., 2016). However, currently, various technologies remain immature in terms of reliability, economy, and eco-friendliness when applied to highly complex contaminated sites (Zhou et al., 2019). For example, the development of green and efficient redox agents and the optimization of injection wells (methods) are not enough to rely on field tests alone (Shi et al., 2020).

Therefore, researchers worldwide are conducting many laboratory investigations to further improve and develop technologies in this regard. To minimize experimental deviations and enhance data reliability, it is important to use homogeneous VOC-contaminated soils (VCSs) as a study object in a laboratory. While it is common to prepare artificially contaminated soils by mixing contaminants with clean base soil, ensuring that the VOCs are homogeneously mixed with the soil can be complicated. A variety of mixing procedures reported in the literature for the preparation of artificial VCSs have been reviewed in Table A1 of the appendix (Ma et al., 2017a, 2017b; Peng et al., 2013; Salman et al., 2015; Shi et al., 2020). These procedures mainly include two kinds of sample preparation modes, free aging of VOCs in soils, and VOC equilibrium via hand mixing. The differences between these existing preparation methods are mainly reflected in the types of pollutants, mixing time, temperature, and mixing equipment employed with each method. As suggested in Table A1, no commonly accepted VCS preparation method is available, considering that even studies in which the same pollutants were investigated showed different preparation temperatures and equilibrium times. Shi et al. (2020) poured benzene into a soil column and allowed the pollutant to diffuse in the sealed column for 8 h at room temperature before the completion of the preparation of the contaminated soil. Ma et al. (2017a) first mixed trichloroethylene (TCE) and water in a volumetric ratio of 100 μL: 10 mL and then mixed the solution with 50 g of soil. They adopted an equilibrium time of 24 h. In another study, Ma et al. (2017b) added a mixture of chloroform (TCM)/TCE in methanol (15 mL: 250 mL) into a wet natural soil sample from the deep ground, after which the mixtures were stirred, compacted, and sealed at 4 °C for the preparation to go to completion. Salman et al. (2015) obtained TCE-contaminated sand via hand mixing. The mixing efficiencies might differ from each other. Meanwhile,

Table 1
Physicochemical properties of various uncontaminated soils.

Property	Test content	Kaolin	Soil 1	Soil 2	Soil 3	Standard/method
Physical properties	Specific gravity (g/cm^3)	2.70	2.23	2.69	2.68	ASTM D854-14; ASTM D4972-13;
	TOC (mg/kg)	0.100	12.3	14.6	8.43	ASTM D4318 - 17e1
	pH	9.21	7.90	5.36	8.22	
	SSA (m^2/g)	8.11	20.2	26.8	15.9	
	Pore volume (cm^3/g)	0.0180	0.0389	0.0551	0.0223	
	Plastic limit (%)	15.2	20.4	28.8	19.8	
	Liquid limit (%)	30.0	37.0	46.2	32.3	
	Plasticity index	14.8	16.6	17.4	12.5	
Main chemical composition (%)	Al_2O_3	33.8	15.2	14.0	16.9	XRF-1800 spectrometer (Shimadzu, Japan)
	SiO_2	42.7	68.8	59.3	65.4	
	Fe_2O_3	5.13	5.63	4.96	5.80	
	CaO	0.410	2.43	7.14	2.20	
	MgO	0.0630	1.29	2.50	2.40	
Mineral composition (%)	Nacrite	/	/	79.3	/	D8-Advance XRD diffractometer (Bruker, Germany); Spectrums were qualitatively and quantitatively by JADE 6.5 with PDF 2004 (International Centre for Diffraction Data, ICDD)
	Rectorite	/	24.8	/	/	
	Quartz	/	72.7	20.7	81.2	
	Albite	/	/	/	18.8	
	Birnessite	/	2.50	/	/	
Particle size analysis	Sand (2000-75 μm)	2.70	61.4	43.3	71.2	ASTM D422-63; ASTM D2487-17;
	Silt (75-5 μm)	63.3	32.0	47.5	27.3	Particle size measured by a laser particle size analyzer (Mastersizer 3000) (Bieganowski et al., 2018)
	Clay (≤5 μm)	34.0	6.60	9.20	1.50	
	Constrained diameter, d_{60}	15.2	451	88.0	366	
	Effective grain diameter, d_{10}	2.30	6.70	5.20	11.8	
	Coefficient of uniformity, C_u	6.60	67.3	16.9	31.0	
	Classification	Lean clay (CL)	Clayey sand (SC)	Sand lean clay	Silty sand (SM)	

different mixing procedures have been reported for the preparation of semi-VOC-contaminated soils. For example, Ren et al. (2020) mixed 3 L *n*-hexane/acetone (v/v = 1:1) containing 60 mL diesel to 1 kg natural soil. The mixtures were left in a fume hood for 24 h so that diesel-contaminated soils could be obtained via the free volatilization of *n*-hexane/acetone. Sawada et al. (2004) observed that mixing with a rotary evaporator or a blender facilitated the preparation of relatively homogenous polycyclic aromatic hydrocarbon-contaminated soils, while hand mixing resulted in extremely high inhomogeneity. The various methods used in the preparation of VCSs indicate that there is no unified or standardized method for the artificial preparation of VCSs.

Therefore, methods for preparing VCSs with excellent homogeneity while ensuring the minimum loss of VOCs during preparation are required. Homogeneity indicates whether the VOCs are evenly distributed in the soil, and it can be determined quantitatively using the coefficient of variation (CV) employed in geo-environmental engineering (Rutkowska et al., 2018; Xia et al., 2019). In contrast, recovery represents the residual amount of VOCs after volatilization (loss) during the preparation process, and it can be determined quantitatively by determining the recovery rate (RR), which is a concept in environmental analytical chemistry (Pulleyblank et al., 2020). However, there is no clear evidence or method to evaluate the homogeneity and recovery of the prepared VCSs, making the effectiveness of mixing methods unknown to other researchers.

Regarding VOC pollution, 74% of the superfund sites in the United States were found to be polluted by VOCs in 1982−2014 (USEPA, 2020). In China, the release of VOCs increases at a drastic rate of 5.9% per year, and a considerable part of the released VOCs ends in the soil (Wei et al., 2011; Zhu et al., 2020). The benzene series (BTEX) and chlorinated hydrocarbons (CHCs) are the most common VOCs in soils (Lin et al., 2019; USEPA, 2020). Moreover, VOCs can also be divided into light non-aqueous phase liquids (LNAPLs) and dense non-aqueous phase liquids (DNAPLs) (Li et al., 2020; Mdlovu et al., 2019). Therefore, toluene, which represents the BTEX and LNAPLs, and perchloroethylene (PCE), which represents CHCs and DNAPLs, were selected as the contaminants for the preparation of the VCSs in this study.

To evaluate the preparation effectiveness of the VCSs prepared using different methods and select the optimal method, six different mixing procedures, based on previous studies (Ma et al., 2017a, 2017b; Ren et al., 2020; Sawada et al., 2004; Shi et al., 2020) were modified and adopted for mixing VOCs with clean kaolin to prepare the VCSs. The CV and RR of the VCSs prepared using the different procedures were determined and compared. Thereafter, the optimal method was assessed using the quantitative AHP-CRITIC-TOPSIS method (Comprehensive evaluation mathematical model; the weight of this model is determined by the combination of subjective weighting method (Analytic Hierarchy Process, AHP) and the objective CRITIC method). Meanwhile, the qualitative evaluation of the various procedures was performed via the determination of phase transformation (free state, adsorbed state, and volatile state) and mass transfer (diffusion, adsorption) during the mixing processes. Furthermore, the practicability and reliability of the optimal mixing method were then validated by using it to prepare VCSs with three natural soil samples. Finally, the factors that affect the adsorption of VOCs onto natural soils, including soil properties, such as total organic carbon (TOC), specific surface area (SSA), pore volume, particle size distribution, pH, plastic limit, mineral composition, and pollutant properties, were discussed to explore the mechanisms of the feasibility of the optimal method.

2. Materials and methods

2.1. Materials

Four base soil types were selected for this study: kaolin was provided by a manufacturer from Xuzhou, China, and the other three were natural soil samples collected from three cities in China: Wuhan (soil 1), Shenzhen (soil 2), and Beijing (soil 3). The specific sampling location and appearance of natural soil samples can refer to Li et al. (2020). All the soils were air-dried and ground in a mortar to pass through a 2-mm mesh. The physicochemical properties of the soils and the corresponding test standards or methods are shown in Table 1. Specifically, the TOC contents of the soils were measured using a Vario TOC analyzer (Elementar, Germany). Their specific surface area (SSA) and pore volume were determined using the BET method with the help of an ASAP 2020 PLUS HD88 analyzer (Micromeritics, USA). Additionally, to determine the mineral compositions of the soil samples, X-ray diffraction (XRD) analysis was performed, and the results obtained are shown in Table 1 and Fig. B1 (appendix).

The physicochemical properties of toluene and PCE (Table B1 in appendix) were determined from International Chemical Safety Cards (0078 & 0076). Toluene (≥99.5%), PCE (≥99.5%), and HPLC-grade methanol (≥99.8%) were purchased from Sinopharm Chemical Reagent Co., Ltd. (Shanghai, China). HPLC-grade dichloromethane (DCM, ≥99.8%) was purchased from Thermo-Fisher (USA). 20 mg of Toluene/PCE was dissolved in DCM to a constant volume (100 mL) to prepare a stock solution (200 mg/L) as a source of soil pollution.

Milli-Q water (Merck Millipore, Germany) was used in this study. The internal standard (25 μg/mL) and surrogate standard (25 μg/mL) used in VOC analysis were supplied by o2si Smart Solutions A LGC Standards Company (Charleston, USA).

Additionally, some common laboratory instruments, including the rotary evaporator (China, RE-5250), hand blender (ROYAL PHILIPS), fume hood (China), laboratory refrigerators (China, 4 °C), glass rods, aluminum boxes (ϕ × h, 8 × 6 cm), and glass beakers, were used in the contaminated-soil preparation process.

2.2. Mixing procedures

It is not conducive for VOCs to be adsorbed onto soil particles or TOC in moist environments, given that most of them are hydrophobic (Kraus et al., 2018). Therefore, air-dry soils were used in mixing procedures. Six procedures (A-F) were used to mix the contaminants into kaolin, and the details are shown in Fig. 1 and Table 2. In general, 100 μL of stock solution was added into 100 g of kaolin to prepare the same initial concentration of contaminated kaolin, but the adding process was different in different methods. As shown in Table 2, these six methods were adapted from previously reported preparation methods (Ma et al., 2017a, 2017b; Ren et al., 2020; Sawada et al., 2004; Shi et al., 2020). Additionally, details related to the parameters that were modified in this study are also listed in Table 2. Because VOCs are active and easy to volatilize, the stirring methods, mixing sequences, and equilibrium conditions were adjusted accordingly.

DCM was adopted as the organic solvent in some methods; its boiling point (39.75 °C) is lower than those of acetone (56.53 °C) and *n*-hexane(69 °C), which have been used as solvents in previous studies (Ren et al., 2020; Sawada et al., 2004). Therefore, it volatilizes faster as an organic solvent, and thus, the volatilization of test pollutants can be reduced. Most procedures were performed at room temperature except for procedures A and C.

In procedure A, the temperature was maintained at 30 °C to reduce pollutant loss caused by the higher temperature under the

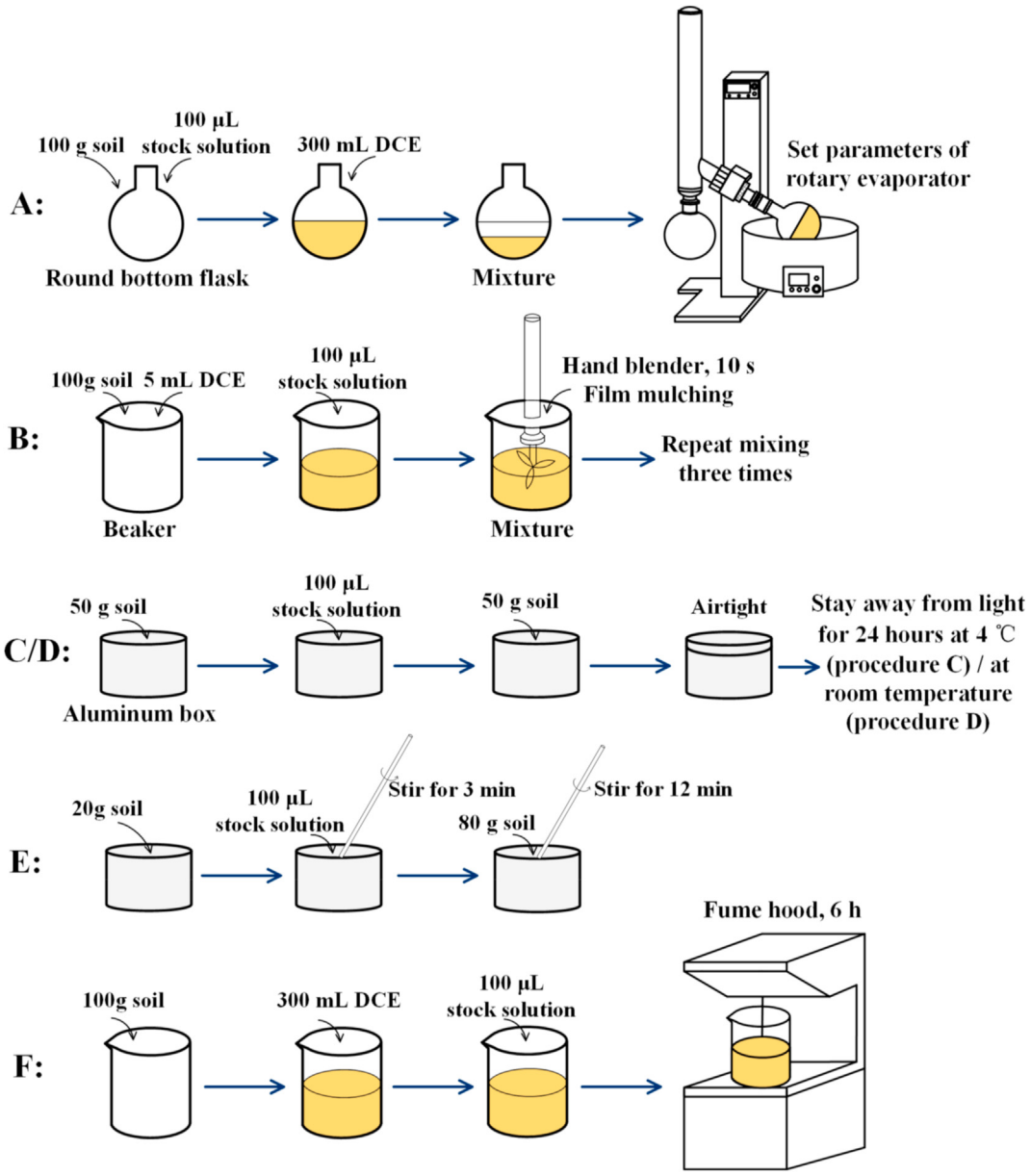

Fig. 1. Display of step by step process for six mixing procedures; except for the temperature specially mentioned in procedure A and C, the other procedures were all kept at room temperature (23 ± 1 °C).

premise of ensuring that a certain amount of the DCM evaporated rapidly. The solid-liquid ratio was set to 1:3. This was to ensure the use of a small amount of solvent while maintaining full contact between the solid and liquid phases. The evaporation time was set to 60 min, which corresponds to the length of time required for the complete volatilization of 300 mL of DCM. In procedure B, the total mixing time was shortened by half (single stirring time was reduced to 10 s and the stirring times were increased) compared to Sawada et al. (2004), owing to the more intense diffusion and volatilization of VOCs. In procedures C and D, the settings were similar to each other, with only the temperature increased from 4 °C to room temperature. For E, the hand mixing stirring times (total 15 min) were close to those corresponding to procedure B, and in procedure F, the solid-liquid ratio (1:3) was set to be consistent with that of procedure A, while the evaporation time was changed to 6 h (DCM volatilization completion).

2.3. Data analysis

Fifteen specimens (each specimen contained 3 g of the contaminated soil) prepared by each procedure were subjected to 7890A gas chromatography-5975C mass spectrometry (GC-MS) (Agilent, USA) as per the USEPA method 8260C and China standard HJ 605−2011. The ambient temperature of the test was maintained at 20 ± 1 °C. The calibration range of the GC-MS test was 50−1000 ng. Therefore, the preset concentration of the contaminated soil was designed to be 200 ng/g, which guaranteed an accurate reading that 3 g of the contaminated soil contained 600 ng of contaminants that were around the midpoint of the calibration curve.

The *P*-values, obtained by performing the *t*-test, were used to describe the probability of error of the measured concentrations of the 15 identical samples. The CV calculated from the determined concentration was defined as the ratio of SD to the arithmetic mean

Table 2
Comparison of the parameters of six mixing procedures used in the paper and parameters referenced from literature; room temperature = 23 ± 1 °C.

Method	Parameters used in the study			Reference parameters				
	Temperature	Soil solvent ratio	Preparation time	Temperature	Soil solvent ratio	Preparation time	Note	References
A	30 °C	Organic solvent, DCM; 1:3 g/mL	60 min	30–35 °C	Organic solvent, acetone; 1:5 g/mL	/	/	Sawada et al. (2004)
				/	Organic solvent, *n*-hexane/acetone (v/v = 1:1); 1:3 g/mL	/	/	Ren et al. (2020)
B	Room temperature	Organic solvent, DCM; 20:1 g/mL	Mixing: 10 s/time, repeated three times	/	Organic solvent, acetone; 20:1 g/mL	Mixing: 30 s/time, repeated twice	/	Sawada et al. (2004)
C	4 °C	/	Aging time, 24 h; Layered pouring of pollutants	Room temperature	/	Aging time, 24 h	/	Ma et al. (2017a)
				4 °C	/	Aging time, 4 d	/	Ma et al. (2017b)
				Room temperature	/	8 h	Layered pouring of pollutants	Shi et al. (2020)
D	Room temperature	/	Same as method C	/	/	/	/	Same as method C
E	Room temperature	/	Hand mixing, 3 min (preparation of 20 g contaminated soil) and 12 min (20 g contaminated soil mixed with 80 g uncontaminated soil)	Room temperature	/	8 h	Layered pouring of pollutants	Shi et al. (2020)
				/	/	/	1000 g homogenized contaminated soil mixed with 5000 g uncontaminated soil	Ren et al. (2020)
F	Room temperature	Organic solvent, DCM; 1:3 g/mL	Aging time, 6 h	/	Organic solvent, *n*-hexane/acetone (v/v = 1:1); 1:3 g/mL	Aging time, 24 h	/	Ren et al. (2020)

(AM) to represent the homogeneity. The specimens were considered to be homogeneous when their CV values were less than 0.05 (Reed et al., 2002). Recovery was determined based on the RR, which was determined according to Eq. (1). An RR greater than 70% suggested a good recovery in the specimen (Pulleyblank et al., 2020).

$$RR = \frac{VOC\ adsorbed\ on\ soils\ after\ mixing}{200\ ng/g} \times 100\% \quad (1)$$

2.4. Comprehensive evaluation model

To evaluate the effectiveness of various mixing methods in this study, we improved and established the AHP-CRITIC-TOPSIS model based on the obtained CVs and RRs (Abdel-Basset and Mohamed, 2020; Zhao et al., 2020). This model reflects the superiority of AHP subjective weighting and fully reflects the data information, making TOPSIS scoring more accurate. The calculation steps were as follows.

Step 1: Determination of evaluation index and classification.

The evaluation indexes were divided into two classes via the AHP, as shown in Fig. E1 (appendix). The weights of first-class indexes (toluene-contaminated kaolin (TCK) and PCE-contaminated kaolin (PCK)) were then determined via subjective weighting.

The CRITIC method was used to calculate the weights of second-class indexes (i.e., CVs of TCK/PCK and RRs of TCK/PCK). The original index matrix $X = (x_{ij};\ i = 1,\ 2,\ \ldots,\ m;\ j = 1,\ 2,\ \ldots,\ n)$ was then constructed by assuming that there are m mixing procedures to be evaluated and n evaluation indexes (second-class indexes).

Step 2: Dimensionless processing of index.

We defined a function that mapped the value of x_{ij} to the interval [0, 1]. A larger value of the index indicates a better evaluation result. In this case, positive dimensionless processing was adopted, as shown in Eq. (2):

$$y_{ij} = \frac{x_{ij} - x_{j,\ min}}{x_{j,\ max} - x_{j,\ min}} \quad (2)$$

Otherwise, the reverse dimensionless treatment was adopted, as shown in Eq. (3):

$$y_{ij} = \frac{x_{j,\ max} - x_{ij}}{x_{j,\ max} - x_{j,\ min}} \quad (3)$$

where $x_{j,\ max}$ and $x_{j,\ min}$ represents the maximum and minimum of the j index, respectively.

In this way, a dimensionless matrix was constructed as $Y = (y_{ij};\ i = 1,\ 2,\ \ldots,\ m;\ j = 1,\ 2,\ \ldots,\ n)$.

Step 3: Calculation of standard deviation and conflict (correlation coefficients).

In the CRITIC method, the standard deviation represents the fluctuation of an index. The larger the standard deviation, the greater the numerical difference of the index, and the more information can be projected. The procedure for calculating the standard deviation is shown in Eqs. (4) and (5).

$$S_j = \sqrt{\frac{\sum_{i=1}^{m} (y_{ij} - \bar{y}_j)^2}{m - 1}} \quad (4)$$

$$\overline{y}_j = \frac{1}{m}\sum_{i=1}^{m} y_{ij} \tag{5}$$

where S_j and $\overline{y}_j$ represent the standard deviation and average value of the j index, respectively.

The correlation coefficient represents the conflict between the indexes, reflecting the similarity between index data information (Abdel-Basset and Mohamed, 2020). The stronger the correlation between a certain index and other indexes, the smaller the conflict between them. The correlation coefficients of the j index were calculated using Eq. (6).

$$R_j = \sum_{j'=1}^{n} 1 - r_{j'j} \tag{6}$$

where $r_{j'j}$ is the correlation coefficient between the j' index ($j' = 1, 2, \ldots, n$) and the j index ($j = 1, 2, \ldots, n$), and R_j represents the conflict value corresponding to the j index.

Step 4: Determination of objective weight and comprehensive weight.

As mentioned before, this weighting method was based on both fluctuation and conflict; thus, they could be expressed according to Eq. (7) as follows:

$$C_j = S_j \sum_{j'=1}^{n} 1 - r_{j'j} \tag{7}$$

where C_j represents the information content contained in the j index.

Therefore, the weights of the j index (W_j) were determined according to Eq. (8) as follows:

$$W_j = \frac{C_j}{\sum_{j=1}^{n} C_j} \tag{8}$$

Meanwhile, the comprehensive weights, CW_j, were obtained by multiplying the subjective weight (first-class indexes, TCK and PCK) and the objective CRITIC weight, W_j (second-class indexes, CVs of TCK/PCK and RRs of TCK/PCK).

Step 5: Normalization of the dimensionless matrix, $Y = (y_{ij};\ i = 1, 2, \ldots, m;\ j = 1, 2, \ldots, n)$

$$z_{ij} = \frac{y_{ij}}{\sqrt{\sum_{i=1}^{m} (y_{ij})^2}} \tag{9}$$

According to Eq. (9), the normalized matrix $Z = (z_{ij};\ i = 1, 2, \ldots, m;\ j = 1, 2, \ldots, n)$ can be obtained. This matrix was processed by performing steps 2 and 5 to convert it into a homotrend matrix.

Step 6: Calculation of decision matrix.

The decision matrix $D = (d_{ij};\ i = 1, 2, \ldots, m;\ j = 1, 2, \ldots, n)$ was obtained by multiplying each column vector of the Z matrix $(z_j;\ j = 1, 2, \ldots, n)$ with its corresponding comprehensive weight, CW_j.

$$D = z_{ij} \times CW_j,\ i = 1, 2, \ldots, m \tag{10}$$

Step 7: Calculation of ideal solution.

The positive ideal solution d_j^+, was obtained using Eq. (11)

$$d_j^+ = \max_{1 \le i \le m} y_{ij},\ j = 1, 2, \ldots, n \tag{11}$$

The negative ideal solution, was obtained using Eq. (12)

$$d_j^- = \min_{1 \le i \le m} y_{ij},\ j = 1, 2, \ldots, n \tag{12}$$

Step 8: Calculation of the distance from row vector (i) to the ideal solution.

Eqs. (13) and (14) represent the distance from the i procedure to the positive/negative ideal solution.

$$g_i^+ = \sqrt{\sum_{j=1}^{n} (y_{ij} - d_j^+)^2},\ i = 1, 2, \ldots, m \tag{13}$$

$$g_i^- = \sqrt{\sum_{j=1}^{n} (y_{ij} - d_j^-)^2},\ i = 1, 2, \ldots, m \tag{14}$$

Step 9: Ranking of various procedures.

The ranking of various procedures was determined via the queuing indicator values (Q_i), which emphasizes the distance from the negative ideal solution, as shown in Eq. (15). The larger the queuing indicator value, the better the procedure.

$$Q_i = \frac{g_i^-}{g_i^+ + g_i^-},\ i = 1, 2, \ldots, m \tag{15}$$

3. Results and discussion

3.1. Homogeneity and recovery of contaminated kaolin

The homogeneity and recovery of the artificial VOC-contaminated kaolin (VCK) prepared via different procedures were compared and shown in Fig. 2, Table C1, and Table C2 (appendix). The P-value of the measured concentrations of each procedure was calculated, and all procedures had P-values < 0.05 (the maximum was 0.0317, which corresponded to TCKs prepared via procedure D).

In Fig. 2a, the split violin plot shows the concentration distribution of toluene/PCE in kaolin. It is evident that the measured concentrations varied significantly with the different mixing procedures; the olive solid lines represent the mean values, and the violet dashed lines represent the median values. The violin plot displays the distribution status and probability density of the data. Among the six procedures, the concentrations measured following procedures C and A were relatively closer to the preset concentration. Comparatively, those measured from samples prepared using procedure E were much lower than the preset values. This might result from the massive amount of volatilization that occurred during hand mixing. Meanwhile, it was observed that the mean and median values of the PCE concentration were slightly higher than those of the toluene concentration, suggesting that the types of contaminants may also affect the mixing efficiency. Importantly, the violin plot was wider close to the mean values, indicating that the data distribution was concentrated around these mean values. Compared with other procedures, the data dispersion following procedures A and E were weaker, indicating that the data distribution was very centralized.

Furthermore, the homogeneities were evaluated by the CVs of the measured concentrations. The CVs are shown in Fig. 2b, and the raw data are exhibited in Table C2. The order of homogeneity of the samples from the six procedures was A < E < C < F < B < D for TCKs.

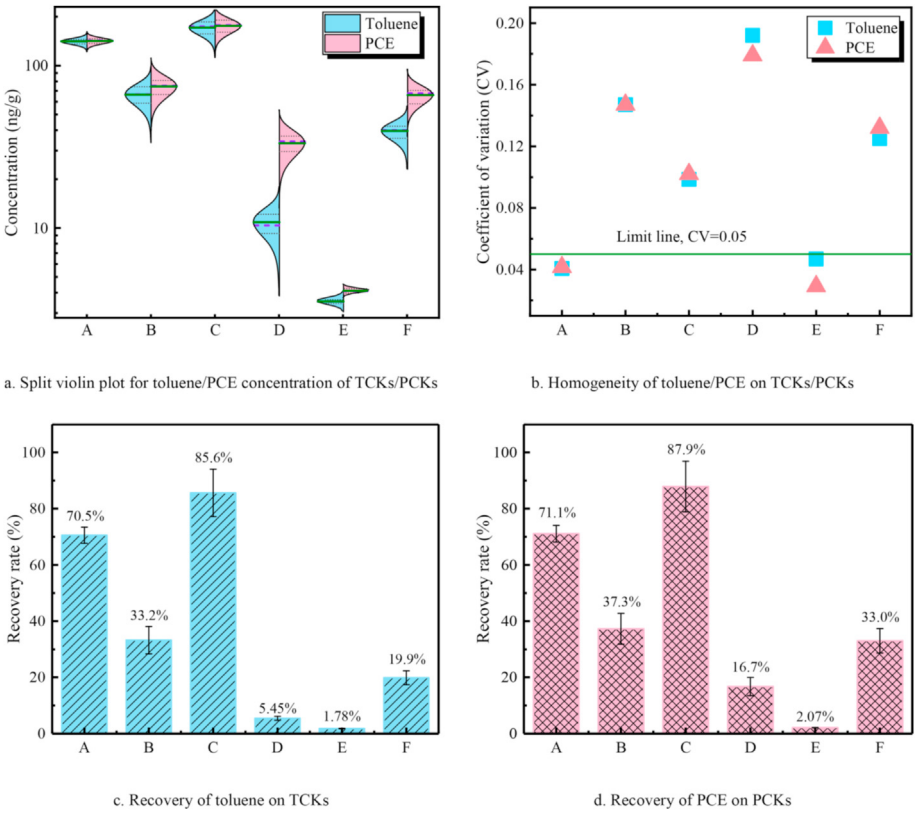

Fig. 2. Concentration distribution, homogeneity, and recovery of toluene/PCE on toluene/PCE-contaminated kaolin (TCK/PCK); in Fig. 2a, the olive solid lines, violet dash lines, and black dot lines represent mean, median, quartiles (25% and 75%) values, respectively. (For interpretation of the references to colour in this figure legend, the reader is referred to the Web version of this article.)

For the PCKs, it was E < A < C < F < B < D. According to Table C2, the CVs of the samples prepared using procedures A and E were all below 0.05 for toluene and PCE, indicating great homogeneity. The CVs of concentrations measured from the other VCKs were all above the 0.05 threshold. Except for procedure E, where the CV of PCK was smaller than that of TCK, all the procedures resulted in poorer PCK homogeneities than those of the TCK. Nevertheless, these findings suggested that procedures A and E produced homogeneous pollutant distribution that was preferred in the laboratory preparation of artificial VCK.

As shown in Fig. 2c and d, there were significant differences (RRs ranging from 1.78 to 87.9%) in contaminant recovery in the soils prepared using the different procedures. The order of the RRs was determined as: C > A > B > F > D > E for both TCKs and PCKs. The RRs of samples prepared using procedures C and A (above 70%) were much higher than those prepared using the other procedures. On the contrary, the recovery of VCK prepared using procedure E was below 5%, indicating that most of the pollutants added were lost after the preparation procedure. Meanwhile, there were no notable differences between the RRs of the two contaminants, regardless of the procedures adopted.

3.2. Mixing method evaluation

Based on the CVs and RRs resulting from the different mixing methods, quantitative and qualitative analyses were further discussed to determine the optimal method.

For quantitative evaluation, the different mixing methods were scored and queued according to the AHP-CRITIC-TOPSIS model (Eqs. 2–15 in section 2.4). The control group consisted of the CV and

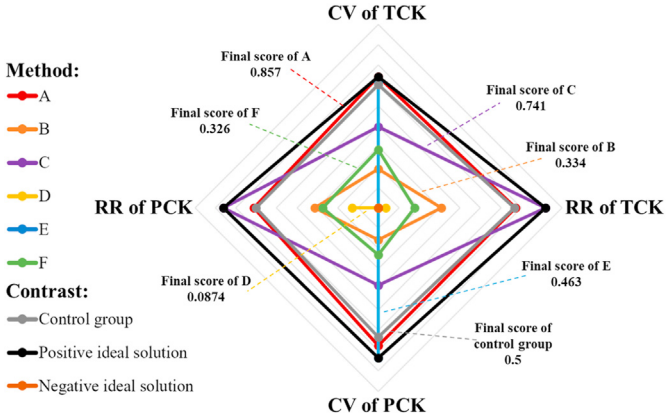

Fig. 3. Radar chart of various methods determined by AHP-CRITIC-TOPSIS model; CV and RR represent the coefficient of variation and recovery rate, respectively; TCS and PCS represent the toluene-contaminated soil and PCE-contaminated, respectively.

RR limit values (i.e., CV = 0.0.5 and RR = 70%). A score that was higher than that of the control group was considered to have good applicability. Fig. 3 and D1, and Table D.1-D.4 (appendix) show the evaluation system and the main results of the quantitative model. The dimensionless processing of the RRs was performed using Eq. (1), and the dimensionless processing of the CVs was performed using Eq. (2), as shown in Table D1. The weights of first-class indexes were determined by the subject weighting method (VOC types should not affect selecting the optimal preparation method; therefore, the weight is the same, which was 0.5). The weights of

second-class indexes were determined using the CRITIC method by executing Eqs. (3)–(7), and comprehensive weights were obtained by multiplying the two-class indexes, as shown in Table D2. Furthermore, the dimensionless matrix was normalized using Eq. (8), and then the decision matrix was obtained using Eq. (9), as shown in the "Normalization and weighting" data in Table D.4. The decision matrix was determined using Eqs. (10) and (11) to obtain positive and negative ideal solutions, as shown in Table D.3. Fig. 3 shows the data corresponding to the decision matrix and the ideal solution based on the radar chart. The closer the enclosed area of each method to that of the positive ideal solution, the better the method is. Finally, the scores of all the methods were determined using Eqs. 12–14 were in descending order: A > C > Control group > E > B > F > D, as shown in Fig. 3 and Table D.4. The larger the queuing indicator value, the better the method.

Reportedly, homogeneity and recovery can be affected by the mechanisms of interphase mass transfer, i.e., the diffusion and phase change between the free state, adsorbed state, and volatile state of pollutants (Essaid et al., 2015). For example, in procedure A, the pollutant solutions and base soils were fully in contact and were mixed during rotary evaporation. Given that the vapor pressure of DCM is much higher than that of toluene or PCE (Janvier et al., 2015), DCM preferentially volatilized under the test conditions. Thus, the pollutants that were dissolved in DCM were first distributed on kaolin as a mobile phase. After DCM volatilization, the pollutants were more evenly diffused and adsorbed onto the kaolin, which contributed to the homogeneity. Further, the pollutant loss in this procedure was relatively low, and the RR value reached 70.5%. In procedure B, it was observed that the hand blender could not completely mix the contaminated soils that were close to the beaker wall, resulting in poor homogeneity. Moreover, it was also observed that several pollutants and clay particles escaped from the beaker due to high-speed rotation. The contaminated soils prepared using this procedure still exhibited a higher RR than those prepared using procedures D, E, and F, owing to the reasonable mixing time. Pollutant diffusion is affected by pore characteristics (Balseiro-Romero et al., 2018). Therefore, the slightly lower homogeneity of the contaminated soils prepared using procedure C compared with those produced using procedures A and E resulted from the slower molecular motion at 4 °C (Nagy, 2019). Meanwhile, the vapor pressure of the pollutant at this temperature was lower than that at room temperature; thus, a less significant volatilization process was expected. Therefore, the RR of the contaminated soil resulting from procedure C was the highest compared to the other procedures performed at room temperature. Comparatively, the room temperature adopted in procedure D resulted in increased molecular motion. The VOC molecules tended to change from the free state to the volatile state at this temperature rather than promote homogeneity via a stable diffusion process. In procedure E, hand mixing at room temperature was adopted, and it resulted in the lowest RR. In procedure F, the DCM in the mixtures was allowed to freely volatilize in a fume hood, leaving the pollutants adsorbed onto the soil particles. However, solids and liquids were stratified in the beaker, and the mixed liquids in the upper layer did not appear fully diffuse and absorb onto the soil particles. Therefore, pollutants preferentially volatilized under the fume hood. Meanwhile, the DCM volatilized during the long preparation time, which led to pollutant loss.

Thus, the optimal method was determined via quantitative calculations and qualitative analyses. Only the scores of procedures A and C were higher than those corresponding to the control group. However, the CVs obtained following procedure C were greater than the limit value. Meanwhile, the interphase mass transfer of procedure A was more conducive for the preparation VCSs with good homogeneity and recovery. Therefore, procedure A is recommended for use in the laboratory preparation of VCSs. Alternatively, while procedure C resulted in a lower homogeneity than procedure A, it showed the highest recovery, and its score was also higher than that of the control group. Additionally, procedure C is simpler and does not require special laboratory equipment, making it more suitable if many contaminated soil samples are required.

3.3. Application of the optimal procedure to natural soils

Procedure A is the optimal mixing method. Further investigations were conducted to validate the applicability of the mixing method when natural soils, rather than kaolin, were used. A comparison of the homogeneity and recovery of the artificial VCSs prepared using the optimal procedure is shown in Fig. 4, Table E1, and Table E2 (appendix). The *P*-values of the measured concentrations were far less than 0.05. In Fig. 4a, the olive solid lines and the violet dashed lines represent the mean and median values of pollutants measured in the artificially contaminated soils prepared from natural soil samples, respectively. In both toluene/PCE-contaminated soils (TCS/PCS), the order of the measured mean concentration values was: soil 2 > soil 1 > soil 3 > kaolin, indicating that soil types and soil properties have an effect on the contaminants adsorbed onto the soil matrix (Lu et al., 2020; Wang et al., 2019; Zytner, 1994). Fig. 4a also revealed that the measured contaminant concentrations in the PCS samples were higher than those in the TCS samples (except soil 3). Importantly, compared with the contaminated soil prepared from natural soil samples, the kaolin-contaminated soil showed a weaker data dispersion, indicating that data distribution was very centralized. Fig. 4b and c, and Table E2 show the homogeneity and recovery of the contaminated soils prepared using the three natural soil samples compared with that prepared from kaolin. In both TCSs and PCSs, the order of CVs was soil 1 > soil 3 > soil 2 > kaolin, suggesting that it is more difficult to reach a perfectly homogenous condition when using natural soils. A comparison between the two pollutants suggested that the homogeneity of PCS was worse than that of TCSs. These results suggest that the homogeneity of the artificial VCSs is dependent on both the soil properties and the pollutant characteristics. Among the tested samples, the CVs of PCS 1 and 3 were 0.0639 and 0.0504, respectively, which were slightly higher than the limit value (0.05). All the other samples had CVs below 0.05. The RRs of the contaminants in the VCSs are shown in Fig. 4c, which shows that all the three natural soil samples resulted in higher RRs than kaolin. Additionally, the RRs of PCS were still higher than those of TCS, except for soil 3, which is consistent with the results from the kaolin group.

These results showed that less homogeneity was associated with the artificial VCSs prepared as per procedure A using the natural soil samples, compared to that prepared from kaolin. In contrast, using natural soils enhanced the RRs of the contaminants. Although the homogeneity of the VCSs prepared using procedure A did not meet the requirement in the two groups (i.e., PCS 1 and 3), the procedure was generally acceptable in terms of homogeneity and contaminant recovery.

The determination of the mixing efficiency using different soils showed that when the same mixing procedure (A) and pollutants are adopted, the homogeneity and contaminant recovery become dependent on soil properties. These properties, including the mineral type and composition, TOC, SSA, pore volume, pH, coefficient of uniformity (C_u), plastic limit, influence the free state diffusion of contaminants and their transformation to an adsorbed state (Li et al., 2020). In this study, the properties of the three natural soils used were different (Table 1), given that they were collected from North, Central, and South China.

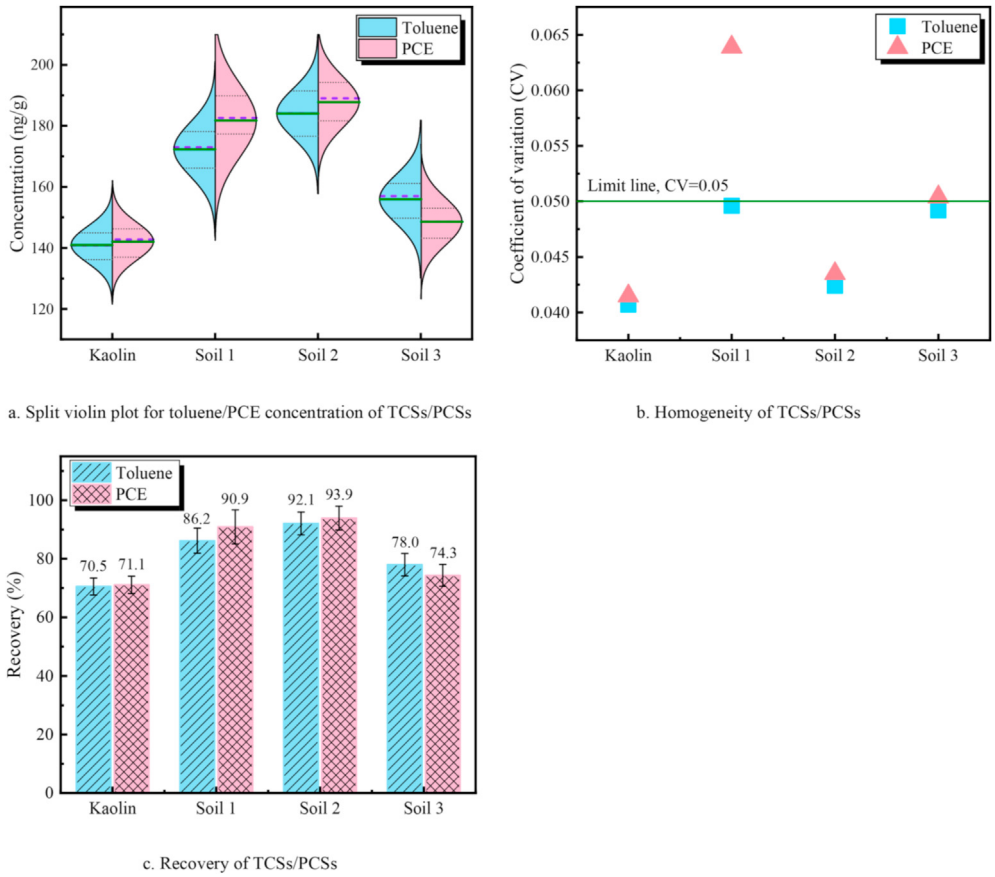

Fig. 4. Effectiveness of natural soils contaminated by procedure A; TCS and PCS represent the toluene-contaminated and PCE-contaminated soil, respectively; the contaminated kaolin is the control group; Fig. 3a shows the concentration distribution of toluene/PCE on soils, the olive solid lines, violet dash lines, black dot lines represent mean, median, quartiles (25% and 75%) values, respectively. (For interpretation of the references to colour in this figure legend, the reader is referred to the Web version of this article.)

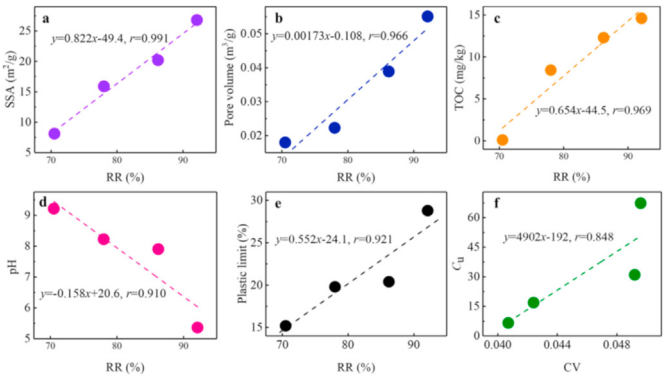

Fig. 5. Some properties of various soils related to the homogeneity and recovery of prepared specimens; r is the correlation coefficient; CV and RR represent the coefficient of variation and recovery rate, respectively.

VOCs can be physically adsorbed on soil particles, and better adsorption of VOCs improves the recovery. As shown in Fig. 5a, the SSA of the soils was found to be closely related to their RRs (linear correlation coefficient $r = 0.991$), i.e., higher SSAs resulted in higher RR values because more physical adsorption sites are available in the soil (Pino-Herrera et al., 2017). Similar effects were observed for the pore volume of the soil samples (Fig. 5b), and the r of pore volume-RRs was 0.966. The tortuous and abundant micropores in the soils possibly provided a large SSA. This enhanced the migration distance and made VOC volatilization difficult. It has also been reported that micropores with lower hydration energy are more favorable for adsorption (Hu et al., 2019). Fig. 5c shows that the TOC contents of the soils are positively correlated with the RRs ($r = 0.969$). Previous studies have demonstrated that hydrophobic organic pollutants can be strongly adsorbed onto soil particles with higher TOC contents (Gondar et al., 2013; Joo et al., 2011; Plaza et al., 2015). This is due to the rich hydrophobic adsorption sites and high SSA of TOC, which allow pollutants like VOCs to be adsorbed on both expanded and condensed domains via the dual-mode model (Martz et al., 2019). Fig. 5d shows that the RRs decreased with soil alkalinity ($r = 0.910$) given that the physical force between the pollutants and soil surfaces (e.g., hydrophobic interaction) becomes weaker as the pH increases (Adeyinka and Moodley, 2019; Ertli et al., 2004). The qualitative and quantitative analyses of the XRD spectra are shown in Fig. B1 and Table 1. It was observed that both soils 1 and 2 contained clayey minerals, 24.8% of rectorite and 79.3% of nacrite, respectively, while soil 3 did not contain clayey minerals. Correspondingly, the order of the RRs from the natural soils was: soil 2 > soil 1 > soil 3. This is because the hydrophobic adsorption sites provided by the clayey minerals in the soils contributed to the RR (Du and Miller, 2007; Hunter, 1981; Yin et al., 2012). The plastic limit (PL), which represents the maximum bound water content of a soil sample, and reflects the ability of the soil to bind water, is a crucial and often used physical parameter of soils (Mitchell and Soga, 2005). Some of the previously mentioned soil properties, e.g., mineral composition and soil pH, can be reflected by the PL value of the soil sample (Andrade

et al., 2011). It has been reported that the adsorption capability of soil is related to its PL value, i.e., the larger the PL, the higher its adsorption capability (Li et al., 2020). Therefore, the PL values of the four soils adopted in this study are shown in Fig. 5e, which indicates a good relationship between PL and RRs ($r = 0.921$).

The coefficient of uniformity (C_u) of soils is commonly used to evaluate the uniformity of soil particles in geotechnical engineering (Du et al., 2016). The larger the C_u, the wider the particle size distribution of the soil, and the more uneven the soil particles (Adeyinka and Moodley, 2019). Such a wider particle size distribution is a natural defect that has adverse effects on the equilibrium process of contaminants in soils. From Fig. 5f, it is evident that the homogeneity of the contaminated soils worsened as their C_u increased (i.e., CV was positively correlated with C_u, $r = 0.848$). Notably, compared to the natural soil samples, the particle distribution of kaolin was relatively more uniform, mainly consisting of fine particles, which explains the better homogeneity. The effect of adsorption on the application of the optimal method can provide a theoretical basis.

Meanwhile, it was observed that when the same procedure and same base soil were used, the homogeneity associated with PCS was worse than that associated with TCS, while a PCS showed the higher RRs. The differences in homogeneity and recovery of the soils contaminated with these two pollutants can be traced back to the differences in their chemical properties. As shown in Table B2, the molecular diameter and relative molecular mass of PCE are more significant than those of the toluene molecule, which limits the molecular thermal motion and molecular diffusion of the contaminants in the soils (Nagy, 2019). Therefore, compared with toluene, it was more difficult for the PCE to be homogeneously distributed in the soils. However, because the vapor pressure of toluene is higher than that of PCE, toluene showed a greater tendency to volatilize and transform from the free state to the volatile state (Gochenour et al., 2018). Moreover, the octanol/water partition coefficient of PCE is higher than that of toluene, making it easier for PCE to be absorbed onto soil particles (Delle Site, 2001). These differences between the two VOCs result in the higher RR values associated with the PCSs.

4. Conclusion

This paper presents a comprehensive study of the effects of different mixing procedures on artificial VCSs. Six different mixing methods for the preparation of toluene and PCE-contaminated kaolin were investigated and evaluated. The selected optimal method was then validated using three different natural soil samples. The main findings of this study are as follows: **(a)** By examining the preparation of contaminated kaolin soil with six procedures, procedures E and A were found to be conducive for optimal homogeneity (CVs were less than 0.05), and in terms of recovery, procedures C and A showed the best results (RRs are larger than 70%). Through the comprehensive mathematical evaluation model (AHP-CRITIC-TOPSIS), procedure A showed the highest score (0.857), and its CVs and RRs were 0.0407/0.0415 and 70.5%/71.1%, respectively. Therefore, procedure A was identified as the best method. **(b)** By applying procedure A to natural soils, the contaminated natural soils showed low homogeneity (CVs, soil 1 > soil 3 > soil 2 > kaolin), but basically met the requirements for application. Additionally, the recovery of these contaminated natural soil was highly varied in the order: soil 2 > soil 1 > soil 3 > kaolin. Therefore, procedure A can be applied to natural soils. **(c)** Whether it is the evaluation of each method or the application analysis for natural soils, the root cause of adsorption of contaminants onto soil particles was the interphase mass transfer, i.e., the phase change between the free state, adsorbed state, and volatile state of pollutants and their diffusion. Moreover, the performance of the contaminated natural soils was related to TOC, SSA, pore volume, pH, C_u, plastic limit, and mineral composition (the correlation was high, $r = 0.848–0.991$), controlled by the adsorption effect. **(d)** Regardless of whether clay or natural soils were used as an object, the homogeneity of PCS was worse than that of TCS; however, it showed better recovery. This is related to the chemical properties of pollutants, e.g., molecular structure, vapor pressure, and octanol/water partition coefficient.

Author contribution

Yuan Li: Investigation, Data curation, Methodology, Writing – original draft. Mingli Wei: Conceptualization, Resources, Writing – review & editing. Lei Liu: Supervision, Writing – review & editing. Bowei Yu: Data curation, Writing – review & editing. Zhiwei Dong: Data curation. Qiang Xue: Supervision, Resources Funding acquisition.

Declaration of competing interest

The authors declare that they have no known competing financial interests or personal relationships that could have appeared to influence the work reported in this paper.

Acknowledgments

This work was supported by the National Science Foundation for Distinguished Young Scholars (grant number 51625903); National Key Research and Development Program (grant number 2019YFC1804002); National Natural Science Foundation of China (grant number51827814, 41702349, 41772342, 41977254); TaoDu elite personal foundation (grant number CX201804C); Youth Innovation Promotion Association CAS (grant number 2017376); Foundation for Innovative Research Groups of Hubei Province of China (grant number 2019CFA012); Wuhan Science and Technology Conversion Special Project (grant number 2018060403011348); and Natural Science Foundation of Hubei Province (grant number 2017CFB203).

Appendix A. Supplementary data

Supplementary data to this article can be found online at https://doi.org/10.1016/j.chemosphere.2021.129571.

References

Abdel-Basset, M., Mohamed, R., 2020. A novel plithogenic TOPSIS-CRITIC model for sustainable supply chain risk management. J. Clean. Prod. 247, 119586.
Adeyinka, G.C., Moodley, B., 2019. Kinetic and thermodynamic studies on partitioning of polychlorinated biphenyls (PCBs) between aqueous solution and modeled individual soil particle grain sizes. J. Environ. Sci-China. 76, 100–110.
Agarwal, A., Liu, Y., 2015. Remediation technologies for oil-contaminated sediments. Mar. Pollut. Bull. 101, 483–490.
Andrade, F.A., Al-Qureshi, H.A., Hotza, D., 2011. Measuring the plasticity of clays: a review. Appl. Clay Sci. 51, 1–7.
Balseiro-Romero, M., Monterroso, C., Casares, J.J., 2018. Environmental fate of petroleum hydrocarbons in soil: review of multiphase transport, mass transfer, and natural attenuation processes. Pedosphere 28, 833–847.
Bieganowski, A., Ryżak, M., Sochan, A., Barna, G., Hernádi, H., Beczek, M., Polakowski, C., Makó, A., 2018. Chapter Five - laser diffractometry in the measurements of soil and sediment particle size distribution. In: Sparks, D.L. (Ed.), Advances in Agronomy. Academic Press, pp. 215–279.
Delle Site, A., 2001. Factors affecting sorption of organic compounds in natural sorbent/water systems and sorption coefficients for selected pollutants. A review. J. Phys. Chem. Ref. Data. 30, 187–439.
Du, H., Miller, J.D., 2007. A molecular dynamics simulation study of water structure and adsorption states at talc surfaces. Int. J. Miner. Process. 84, 172–184.
Du, Y.J., Wei, M.L., Reddy, K.R., Wu, H.L., 2016. Effect of carbonation on leachability, strength and microstructural characteristics of KMP binder stabilized Zn and Pb

contaminated soils. Chemosphere 144, 1033–1042.
Ertli, T., Marton, A., Foldenyi, R., 2004. Effect of pH and the role of organic matter in the adsorption of isoproturon on soils. Chemosphere 57, 771–779.
Essaid, H.I., Bekins, B.A., Cozzarelli, I.M., 2015. Organic contaminant transport and fate in the subsurface: evolution of knowledge and understanding. Water Resour. Res. 51, 4861–4902.
Gochenour, K., Heyert, A.J., Lindberg, G.E., 2018. Chapter 2 - molecular simulations of volatile organic interfaces. In: Faust, J.A., House, J.E. (Eds.), Physical Chemistry of Gas-Liquid Interfaces. Elsevier, pp. 41–58.
Gondar, D., Lopez, R., Antelo, J., Fiol, S., Arce, F., 2013. Effect of organic matter and pH on the adsorption of metalaxyl and penconazole by soils. J. Hazard Mater. 260, 627–633.
Hu, E., Zhao, X., Pan, S., Ye, Z., He, F., 2019. Sorption of non-ionic aromatic organics to mineral micropores: interactive effect of cation hydration and mineral charge density. Environ. Sci. Technol. 53, 3067–3077.
Hunter, R.J., 1981. Chapter 8 - influence of more complex adsorbates on zeta potential. In: Hunter, R.J. (Ed.), Zeta Potential in Colloid Science. Academic Press, pp. 305–344.
Janvier, F., Tuduri, L., Cossement, D., Drolet, D., Lara, J., 2015. Micropore characterization of activated carbons of respirator cartridges with argon, carbon dioxide, and organic vapors of different vapor pressures. Carbon 94, 781–791.
Joo, J.C., Kim, J.Y., Nam, K., 2011. Sorption of nonpolar neutral organic compounds to model aquifer sands: implications on blocking effect. J. Environ. Sci. Heal. A. 46, 1008–1019.
Kraus, M., Trommler, U., Holzer, F., Kopinke, F.-D., Roland, U., 2018. Competing adsorption of toluene and water on various zeolites. Chem. Eng. J. 351, 356–363.
Li, Y., Wei, M., Liu, L., Xue, Q., Yu, B., 2020. Adsorption of toluene on various natural soils: influences of soil properties, mechanisms, and model. Sci. Total Environ. 740, 140104.
Lim, M.W., Lau, E.V., Poh, P.E., 2016. A comprehensive guide of remediation technologies for oil contaminated soil - present works and future directions. Mar. Pollut. Bull. 109, 14–45.
Lin, X., Xu, C., Zhou, Y., Liu, S., Liu, W., 2019. A new perspective on volatile halogenated hydrocarbons in Chinese agricultural soils. Sci. Total Environ. 703, 134646.
Lu, Y., Li, Y., Liu, D., Ning, Y., Yang, S., Yang, Z., 2020. Adsorption of benzene vapor on natural silicate clay minerals under different moisture contents and binary mineral mixtures. Colloids Surf., A 585, 124072.
Ma, Y., Dong, B., He, X., Shi, Y., Xu, M., He, X., Du, X., Li, F., 2017a. Quicklime-induced changes of soil properties: implications for enhanced remediation of volatile chlorinated hydrocarbon contaminated soils via mechanical soil aeration. Chemosphere 173, 435–443.
Ma, Y., Shi, Y., Hou, D., Zhang, X., Chen, J., Wang, Z., Xu, Z., Li, F., Du, X., 2017b. Treatability of volatile chlorinated hydrocarbon-contaminated soils of different textures along a vertical profile by mechanical soil aeration: a laboratory test. J. Environ. Sci-China. 54, 328–335.
Martz, M., Heil, J., Marschner, B., Stumpe, B., 2019. Effects of soil organic carbon (SOC) content and accessibility in subsoils on the sorption processes of the model pollutants nonylphenol (4-n-NP) and perfluorooctanoic acid (PFOA). Sci. Total Environ. 672, 162–173.
Mdlovu, N.V., Lin, K.S., Chen, C.Y., Mavuso, F.A., Kunene, S.C., Carrera Espinoza, M.J., 2019. In-situ reductive degradation of chlorinated DNAPLs in contaminated groundwater using polyethyleneimine-modified zero-valent iron nanoparticles. Chemosphere 224, 816–826.
Mitchell, J.K., Soga, K., 2005. Fundamentals of Soil Behavior, third ed. John Wiley & Sons, Inc., Hoboken.
Nagy, E., 2019. Chapter 4 - molecular diffusion. In: Nagy, E. (Ed.), Basic Equations of Mass Transport through a Membrane Layer, second ed. Elsevier, pp. 69–90.
Pino-Herrera, D.O., Pechaud, Y., Huguenot, D., Esposito, G., van Hullebusch, E.D., Oturan, M.A., 2017. Removal mechanisms in aerobic slurry bioreactors for remediation of soils and sediments polluted with hydrophobic organic compounds: an overview. J. Hazard Mater. 339, 427–449.
Plaza, I., Ontiveros-Ortega, A., Calero, J., Aranda, V., 2015. Implication of zeta potential and surface free energy in the description of agricultural soil quality: effect of different cations and humic acids on degraded soils. Soil. Till. Res. 146, 148–158.
Pulleyblank, C., Kelleher, B., Campo, P., Coulon, F., 2020. Recovery of polycyclic aromatic hydrocarbons and their oxygenated derivatives in contaminated soils using aminopropyl silica solid phase extraction. Chemosphere 258, 127314.
Reed, G.F., Lynn, F., Meade, B.D., 2002. Use of coefficient of variation in assessing variability of quantitative assays. Clin. Diagn. Lab. Immunol. 9, 1235–1239.
Ren, J., Song, X., Ding, D., 2020. Sustainable remediation of diesel-contaminated soil by low temperature thermal treatment: improved energy efficiency and soil reusability. Chemosphere 241, 124952.
Rutkowska, M., Kochańska, K., Kandel, L., Bajger-Nowak, G., Słomińska, M., Marć, M., Chojnacka, K., Polkowska–Motrenko, H., Zabiegała, B., Namieśnik, J., Konieczka, P., 2018. Homogeneity study of candidate reference material (contaminated soil) based on determination of selected metals, PCBs and PAHs. Measurement 128, 1–12.
Salman, M., Gerhard, J.I., Major, D.W., Pironi, P., Hadden, R., 2015. Remediation of trichloroethylene-contaminated soils by star technology using vegetable oil smoldering. J. Hazard Mater. 285, 346–355.
Sawada, A., Kanai, K., Fukushima, M., 2004. Preparation of artificially spiked soil with polycyclic aromatic hydrocarbons for soil pollution analysis. Anal. Sci. 20, 239–241.
Shi, J., Yang, Y., Li, J., Xi, B., Wang, Y., Wang, Y., Tang, J., 2020. A study of layered-unlayered extraction of benzene in soil by SVE. Environ. Pollut. 263, 114219.
Tan, X., Chen, Y., Xue, Q., Wan, Y., Liu, L., 2020. Conditioning of resuspension excess sludge with chemical oxidation technology: the respective performance of filtration and expression stage in compression dewatering. Separ. Purif. Technol. 237, 116317.
USEPA, 2020. Superfund Remedy Report, sixteenth ed. U.S. Environmental Protection Agency, Office of Land and Emergency Management. EPA-542-R-20-001. July 2020.
Vidonish, J.E., Zygourakis, K., Masiello, C.A., Sabadell, G., Alvarez, P.J.J., 2016. Thermal treatment of hydrocarbon-impacted soils: a review of technology innovation for sustainable remediation. Eng. Times 2, 426–437.
Wang, B., Zeng, D., Chen, Y., Belzile, N., Bai, Y., Zhu, J., Shu, J., Chen, S., 2019. Adsorption behaviors of phenanthrene and bisphenol A in purple paddy soils amended with straw-derived DOM in the West Sichuan Plain of China. Ecotoxicol. Environ. Saf. 169, 737–746.
Wei, W., Wang, S., Hao, J., Cheng, S., 2011. Projection of anthropogenic volatile organic compounds (VOCs) emissions in China for the period 2010–2020. Atmos. Environ. 45, 6863–6871.
Xia, W.-Y., Du, Y.-J., Li, F.-S., Guo, G.-L., Yan, X.-L., Li, C.-P., Arulrajah, A., Wang, F., Wang, S., 2019. Field evaluation of a new hydroxyapatite based binder for ex-situ solidification/stabilization of a heavy metal contaminated site soil around a Pb-Zn smelter. Construct. Build. Mater. 210, 278–288.
Xu, C., Lin, X., Yin, S., Liu, K., Liu, W., 2019. Spatio-vertical characterization of the BTEXS group of VOCs in Chinese agricultural soils. Sci. Total Environ. 694, 133631.
Yin, X., Gupta, V., Du, H., Wang, X., Miller, J.D., 2012. Surface charge and wetting characteristics of layered silicate minerals. Adv. Colloid. Interface. 179–182, 43–50.
Zhao, D., Li, C., Wang, Q., Yuan, J., 2020. Comprehensive evaluation of national electric power development based on cloud model and entropy method and TOPSIS: a case study in 11 countries. J. Clean. Prod. 277, 123190.
Zhou, Z., Liu, X., Sun, K., Lin, C., Ma, J., He, M., Ouyang, W., 2019. Persulfate-based advanced oxidation processes (AOPs) for organic-contaminated soil remediation: a review. Chem. Eng. J. 372, 836–851.
Zhu, L., Shen, D., Luo, K.H., 2020. A critical review on VOCs adsorption by different porous materials: species, mechanisms and modification methods. J. Hazard Mater. 389, 122102.
Zytner, R.G., 1994. Sorption of benzene, toluene, ethylbenzene and xylenes to various media. J. Hazard Mater. 38, 13–126.